Design and experiments of 4CJ-1200 self-propelled tea plucking machine

Yu Han, Hongru Xiao, Zhiyu Song*, Qiaomin Chen, Wenqin Ding, Song Mei

(*Nanjing Research Institute for Agricultural Mechanization Ministry of Agriculture and Rural Affairs, Nanjing 210014, China*; *Key Laboratory of Modern Agricultural Equipment, Ministry of Agriculture and Rural Affairs, Nanjing 210014, China*)

Abstract: As agricultural labor is decreasing, famous tea production is nearly hard to sustain and is getting more and more expensive in China. To improve the mechanization of tea plucking, this paper designs a self-propelled track-type tea plucking machine that integrates mechanic, hydraulic and electronics. The main parameters of chassis were optimized based on conditions of tea garden. And, three different kinds of cutter blades were designed and analyzed about vibration performance with finite element software. Also, a rigid-flex mixed motion model was established. Based on the model and plots, it is explicit that: 1) the blades move in a sine law; 2) the blades take a symmetrical deform from middle to end while moving; 3) the deformation increases along the blade from the center to sides. The single factor experiment revealed that both travel speed and speed ratio of cutting and travelling had a significant effect on quality indexes (integrity rate, unpicking rate, stubble unevenness) of plucked tea leaf. By universal rotary combination experiment of quadratic regression, the regression equations of three indexes about two experimental factors were established. And, the comprehensive optimization of three indexes was conducted with software Design expert. The optimal operating parameters of machine are as follow: travel speed is 0.41 m/s, speed ratio of cutting and travelling is 1.06; prediction of three indexes are that integrity rate could be reach to 78.26%, unpicking rate reduced to 0.82%, stubble unevenness reduced to 1.30 mm. The results of verification experiment are that: integrity rate could be reach to 77.41%, unpicking rate reduced to 0.87%, stubble unevenness reduced to 1.23 mm. These test indexes that are very close to the predicted values, all surpass the requests specified in the standard of tea plucking with machine. In all, the optimized parameter set is indeed synthetically optimal one that enables the wide use of this tea plucking machine, which can be used in the tea garden that has a lengthways slope less than 18°, a crosswise slope less than 20°, and a height of tea trees between 50-120 cm. From above, the tea plucking machine investigated in this paper provides an effective solution to present tea picking problem that is the bottleneck of tea industry. Further studies need to do for making this machine more automated and intelligent.

Keywords: agricultural machine, tea, harvesting, reciprocating cutter, model, design, experiment, optimization
DOI: 10.25165/j.ijabe.20211406.5519

Citation: Han Y, Xiao H R, Song Z Y, Chen Q M, Ding W Q, Mei S. Design and experiments of 4CJ-1200 self-propelled tea plucking machine. Int J Agric & Biol Eng, 2021; 14(6): 75–84.

1 Introduction

As we know, tea should be plucked timely while it is mature, or the nutrition would be consumed for growth, leading a bad quality[1,2]. And there is a rather short period for plucking, usually less than 7 d. Traditionally, tea plucking needs mass of human labors. As the development of society, the labor for agriculture is decreasing sharply. Therefore, tea plucking machine is much needed and will provides basic support for tea production in China and other tea producing areas.

The mechanization of tea plucking has only been investigated for several years. Relative investigations are mainly about design and kinematics analysis of tea plucking cutter, and mechanical and physical properties of tender tea sprouts[3-7]. Traditional tea plucking machine used in China and other producing area are mainly imported from Japan. These machines[8-11] can be classified into two types by their driving power: electrical motor and gasoline engine, and into three types by move mode: carried by single person type (refer to single-type), carried by du-person type (refer to du-type) and self-propelled type, which all pluck tea shouts down from the tree's crown, but cannot control the length and tenderness of plucked tea sprouts to meet the requirement of Chinese famous tea. The typical single-type includes 4CD-20 (electrical), 4CD-330 NV45H, AM-100E, ML-500, etc. The typical du-type includes 4CSW910, 4CSW-1000, PHV-100, V New Z-1000 etc. These tea plucking machines cannot be used for famous tea plucking, because these machines cut tea sprouts without selecting. Recently, Wu[12] developed a handle controlled self-propelled tea plucking machine, which promoted the productivity to some extent, but not be used widely. Japan has a rather developed mechanization of tea producing; a widely used tea plucking machine is a self-propelled ride type one[13], which makes plucking more automatic and efficient. However, due to plucking without selectivity ether, this machine can just be used for plucking

Received date: 2020-11-10 **Accepted date:** 2021-08-12
Biographies: Yu Han, PhD candidate, research interests: automatic and intelligent plucking equipment for tea, Email: changda_2008@126.com; **Hongru Xiao**, Research Fellow, research interests: agricultural mechanization equipment; **Qiaomin Chen,** Research Fellow, Director, research interests: agricultural mechanization equipment, Email: nnncqm@163.com; **Wenqin Ding,** PhD candidate, Associate Research Rellow, research interests: automatic agricultural equipment, Email: dingwq1987@126.com; **Song Mei,** PhD candidate, Research Assistant, research interests: automatic agricultural equipment, Email: Meisong100@126.com.
***Corresponding author: Zhiyu Song,** PhD candidate, Associate Research Rellow, research interests: agricultural mechanization equipment. Nanjing Research Institute for Agricultural Mechanization, Nanjing 210014, China. Tel: +86-15366093037, Email: songzy1984@163.com.

bulk tea but not famous tea; and it is not be widely used in China and other tea producing area for its' inexpensiveness and the difference of cultivation of agricultural among different countries and areas.

Tea harvesting has always been tedious work in domestic tea planting areas in tea plucking season. To improve the high-efficiency mechanization of high-quality tea plucking for China's tea garden, this paper designs a self-propelled track-type tea plucking machine, which is suitable for domestic tea garden with gentle slope. In order to improve the integrity rate, the experiments were conducted in a tea garden to optimize parameters and obtain the comprehensive optimization of them. The research provides an efficient mechanical equipment for the high-quality tea plucking in tea gardens with gentle slope, which can effectively alleviate the current labor pressure of tea plucking.

2 General structure and working principle

2.1 General structure and working principle

The tea plucking machine adopts the principle of arc-type double-blade reciprocating cutting, which mainly consists of a track chassis with a hydraulic system, frame assembly, plucking system, leaf collecting system, power transmission system, cutter elevating system, and so on. The general structure is represented in Figure 1. The frame assembly (2) and the rubber tracker (1) comprise the main body of the machine; the cutter (3), blast pipe (4), plucking motor (12) and collecting bags are fixed on the escalator (15) that is hinged to the sprocket chain of the elevator mechanism (16) in four vertices; and the blast pipe (4) is connected to the draught fan (7) by a flexible pipe and directs the wind upward to the cutter (3) to collect the plucked sprouts. While working, the machine rides on the tea trees, the cutter is situated on the top surface of the tea trees and plucks the tea sprouts. The plucked tea leaves are collected to the collecting bags with the help of draught fans. A collection box is provided for storing plucked tea sprouts. The height of the elevator system[14] can be adjusted by a motor to obtain a proper relative position of the cutter to the tree surface, which guarantees the plucking quality.

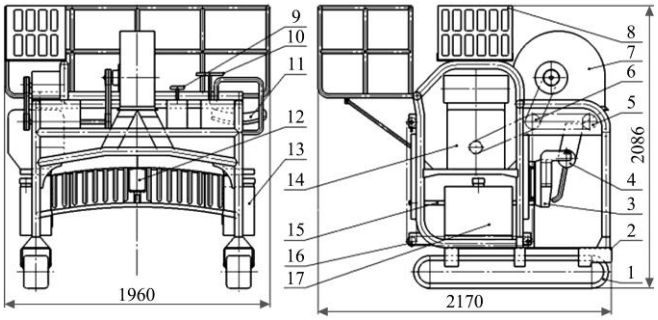

a. Front view b. Left view

1. Track 2. Frame 3. Cutter 4. Blast pipe 5. Hydraulic pump 6. Driveline 7. Fan 8. Tea collector 9. Joystick 10. Direction handle 11. Seat 12. Hydraulic motor 13. Reservoir 14. Engine 15. Elevating carrier 16. Elevating mechanism 17. Gasoline tank

Figure 1 Drawing of self-propelled tea plucking machine

2.2 Main parameters and technical indicators

The row pitch of domestic tea gardens is about 1400-1800 mm, the distance of adjacent tee trees is about 300-400 mm, the height of tea trees is about 600-1100 mm, and the breadth of the tea crown is 1.1-1.3 m[15]. Based on the actual situation of most tea gardens in the national tea area, the main parameters and technical indicators of this tea machine are listed in Table 1.

Table 1 Main technical parameters of the machine

Parameter	Value
Installation dimensions (length×width×height)/mm	2170×1960×2086
mass/kg	750
Distance between tracks/m	1.5
ground clearance	50-100
Cutting width/m	1.2
Matched power/kW	20-25 (GX690)
Fan power/kW	1.1
Productivity/kg h^{-1}	300
Work row Number	1
Intact Rate	≥70%
Unpicking Rate	≤2%
Stubble Roughness	≤4%
Plucking standard	one bude with 1-3 leaves
Cutter displacement control mode	Electronical

3 Design and analysis of main components

3.1 Track chasis

The main parameters of the chassis were designed according to empirical equations based on the determined preliminary parameters of the machine and the cultivating parameters[16]. The mass of the machine is 800 kg. For low-speed vehicles, it is advisable to adopt caterpillar structures with the utilization of no approaching and leaving angle[17].

3.1.1 Main parameters of the chasis

Passing performance includes turning characteristics, ground attachment characteristics, and the main chassis parameters that affect these characteristics are the length of the track's ground-contact fraction, track gauge, and track width. For viscous soils, the track's allowable sinking is limited or driving resistance is increased sharply. Scilicet, the track's ground contact pressure, must be less than the tolerated value[18,19]. Generally, the projection of the center of gravity of the machine on the ground does not coincide with the geometric center of the square formed by the portion of the track connected to the ground, so the ground contact pressure of the track is generally linear, and the maximum value reflects the actual passing performance and working stability of the machine[18,19]. In this paper, the maximum ground contact pressure of straight-line driving, turning, and working conditions is taken as the objective function. The steering parameters, the core area of the track ground contact area and the planting conditions of the tea plantation are used as constraints to nonlinearly plan the chassis parameters. The objective function and the constraint condition are expressed as Equation (1)[15,16].

$$P_{\max}(G,b,L,C,B,e)=\frac{10G}{2bL}(1+\frac{2C}{B})(1+\frac{6e}{L})$$

$$\begin{cases}0.6\le\dfrac{L_0}{B}\le1.3\\ 0.18\le\dfrac{b}{L_0}\le0.22\\ L_0\approx1.073\sqrt[3]{G}\\ L=L_0+2\times0.143\\ 0\le C\le\dfrac{B}{2}\\ 0\le e\le\dfrac{L}{6}\end{cases}\quad(1)$$

where, $P_{\max}$ is maximum ground contact pressure of the track, kPa;

G is the mass of the whole machine, kg; b is the track width, m; L is the length of the track's ground-contact fraction, m; C is the lateral eccentricity of the projection of the center of gravity of the machine in the geometric center of the square formed by the portion of the track connected to the ground, m; e is the longitudinal eccentricity of the projection of the center of gravity of the machine in the geometric center of the square formed by the portion of the track connected to the ground, m; L_0 represents the track gauge (the distance between the drive wheel and the guide wheel), m.

When the value of G is 800 kg (including the driver's mass), the approximate value 0.996 of L_0 can be obtained from the empirical Equation (1). In order to optimize the main parameters of the chassis, according to the optimization theory, a small neighborhood was extended, taking variation range of L_0 to be from 0.8 to 1.1 m; The common planting distance varies from 1.4 to 1.8 m, so the variation range of B is from 1.4 m to 1.8m, and the range of other variables is determined by the inequality constraint.

Optimizing the above-mentioned constrained nonlinear problem with the *fmincon* function in Matlab, the optimal parameters are $[b, L, C, B, e] = [0.1429, 1.08, 0.4006, 1.6024, 0.09]$, and the maximum ground contact pressure is 1.3892 kPa. According to the optimization results, the selection and design parameters are as follows: $[b, L, C, B, e] = [0.15, 1.1, 0.4, 1.6, 0.1]$. The eccentricity of the center of gravity of the machine in the core area of the plane is guaranteed to be less than (0.4, 0.1).

In China, tea gardens are mostly distributed in the hilly and mountainous areas of the south where the climate is humid and the soil moisture content of tea gardens is large. Most mature tea gardens are no-tillage all year round, thus the soil layer is relatively tight. According to the soil classification in the theory of engineering machinery chassis, the soil mechanical properties of tea gardens can take the uncultivated fine sand land[13] (anti-sinking coefficient: 4903.3-5883.9 kPa/m; maximum allowable specific pressure p'_{max}: 588.40-688.47 kPa; driving resistance coefficient: 0.1; adhesion coefficient: 0.45-0.55). Substituting the data into Equation (1) can obtain the maximum grounding specific pressure of 1.53 kPa, which is much smaller than the allowable grounding specific pressure of tea garden soil (wet clay, ploughed soil), and the design parameters of the track meet the requirements.

The main parameters calculated by the empirical equation[16,17] are as follows. L_0: 0.814 m, L: 1.1 m, B: 1.6 m, b: 0.15 m, t_0: 0.072 m, D_k: 0.144 m, D_t: 0.117 m, d_z: 0.117 m, L': 2.532 m.

3.1.2 Analysis of slope adaptability

1) Slope angle

The displacement hydraulic motor of this machine is 229.2 mL/r, the maximum speed is 90.3 r/min, the rated pressure is 16 MPa, and the rated driving force is calculated to be F=2578.87 N. As shown in Figure 2, traveling on the slope is required to overcome slope resistance G_x, rolling resistance F_y and air resistance F_n. Low-speed driving does not count air resistance, and if the slope angle is α, it should be satisfied $F \geq F_y + G_x = f G + G \sin\alpha$, so yield that α should less than 18.8 °.

2) Anti-tilt angle

When the moment of machine's gravity component with slope is greater than the moment generated by the vertical component of gravity, machine will tip. The longitudinal and lateral eccentricity of gravity take the maximum value of the optimization allowable range, that is, e = 0.1 m, C = 0.4 m. The large-mass parts are arranged in the lower part of the machine, so the height h of the center of gravity is half of the height of the whole machine. The conditions for the vertical and horizontal slopes are: $G \sin\alpha \cdot h < G \cos\alpha \cdot (0.5L - e)$ and $G \sin\beta \cdot h < G \cos\beta \cdot (0.5B - C)$. The anti-tilt angles are 23.34 °and 20.98 °respectively.

In all, the optimized parameter can be used in the tea garden that has a lengthways slope less than 18 °, a crosswise slope less than 20 °.

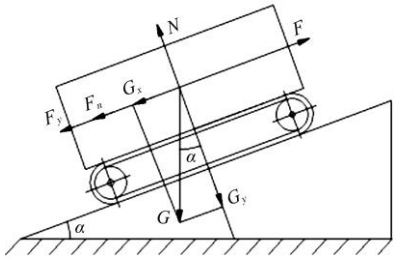

Note: F is drive force; N is reacting force; G is gravity; G_x is the slope resistance (gravity component with slope); G_y is the vertical component of gravity; F_y is the rolling resistance; F_x is the air resistance; α is the slope angle, (°); f is the rolling resistance coefficient. (Force unit: N)

Figure 2 Machine's force diagram on the slope

3.2 Improvement and motion analysis of the cutter

3.2.1 General structure of the cutter

The structure of the cutter is shown in Figure 3. Figure 3a shows the overall perspective of the cutter; while Figure 3b is the inner structure of the cutter drive mechanism. It mainly consists of two blades (7 and 12), a movement positioning plate for the blade (1), a double eccentric wheels shaft (3), the bears (4, 5, 9, and 10) and a cutter box (2 and 11). The connecting bats (6 and 8) for the driving of blades are appropriately matched with the double eccentric shaft, between which bears are installed. With an eccentric distance between two wheels of the shaft, the blades would have a reciprocating motion while the shaft driven by the motor starts spinning. The reciprocating distance is equal to the eccentric distance of the shaft[20].

a. Overall perspective

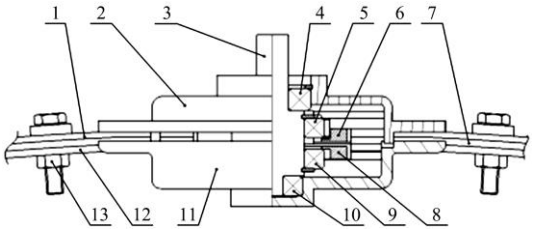

b. Inner structure of the cutter drive mechanism

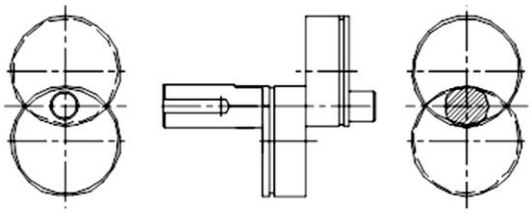

c. Double eccentric wheels shaft

1. Movement positioning plate for blade 2. Upper box of cutter 3. The double eccentric shaft 4. Upper bear in the double eccentric shaft 5. Bear in Upper eccentric wheel 6. Connecting bat for driving of up blade 7. Upper blade 8. Connecting bat for driving of down blade 9. Bear in down eccentric wheel 10. Down bear in the double eccentric shaft 11. Down box of cutter 12. Down blade 13. Bolt for restricting displacement.

Figure 3 Inner structure of cutter

3.2.2 Optimization of arch blade

At present, the common arc-shape blade drive shaft is located at one end of the blade. The disadvantages are as follows: 1) low transmission efficiency; 2) motor offset, which makes the center of gravity of the machine deviate from the core area of the track plane, reducing the traveling performance of the whole machine; 3) the deformation of the blade, the uneven force and wear, and the life principle is not met. Vibration characteristics are the main quality of the cutter, which affects the life of the cutter and the quality of the picking. The vibration characteristics of the blade are related to the restraint position[21-23], which is related to the position of the blade drive shaft. So, three blades with different position of driving shaft (the distance between the drive shaft and the end of the blade are 0 mm, 300 mm, and 600 mm respectively) are analyzed and compared. The structures are shown in Figure 4 and Table 2.

By analyzing the constrained modes on three kinds of blades with the finite element analysis software Patran & Nstran, the first ten modes array and natural frequency can be obtained[24,25]. The first four modes of the three blades are shown in Figure 5. It can be seen that the greater the distance between the free end and the fixed end, the larger amplitude of the main vibration: blade 1>blade 3>blade 2. The first four main frequencies of the blade 1 to 3 are 1.43, 5.03, 8.0, 23.7 Hz, 5.47, 5.49, 30.04, 35.78 Hz, and 2.38, 10.71, 14.18, 24.60 Hz. Because of the varieties of tea, the cutting speed of the tea cutter is from 750 to 1200 r/min and the frequency range is from 12.5 to 20 Hz[7]. The third and fourth mode frequencies of blade 1 are close to the range. The third main frequency of blade 3 is within the driving frequency range but that of blade 2 avoids the driving frequency range. When the driving frequency is close to or coincides with the natural frequency of the structure, resonance[26-29] will affect the picking quality and blade's life, so blade 2 was selected.

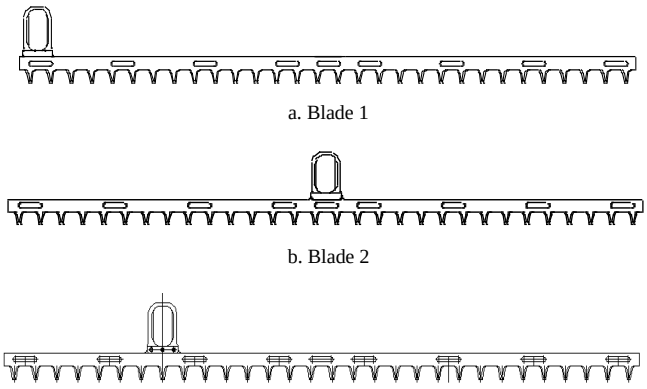

a. Blade 1

b. Blade 2

c. Blade 3

Figure 4 Three kinds of blades with different actuator position

Table 2 Parameters of new blade

Radius *r*/mm	Arc length *l*/mm	Blade thickness *d*/mm	Tooth height *h*/mm	Tooth intervals *s*/mm	Tooth number	Milling angle *α*/(°)	Edge angle *β*/(°)	Front edge angle *γ*/(°)	Front edge *b*/mm
1200	2.5	2.5	22	40	30	20	30	45	6

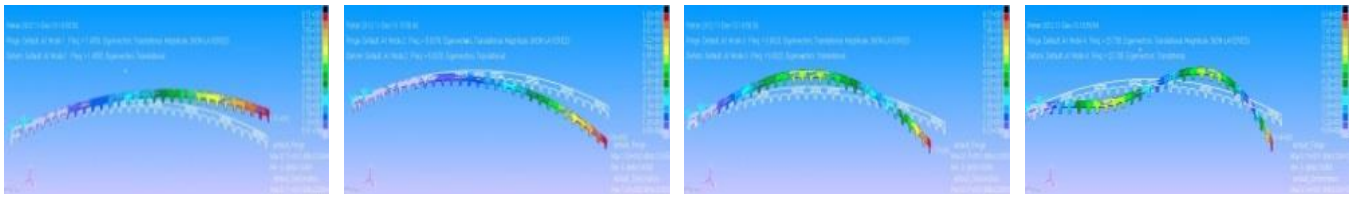

First-order mode Second-order mode Third-order mode Fourth-order mode

a. First four modes of the blade 1

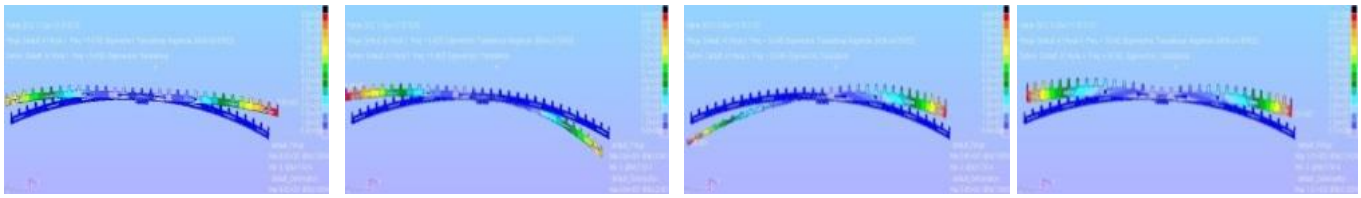

First-order mode Second-order mode Third-order mode Fourth-order mode

b. First four modes of the blade 2

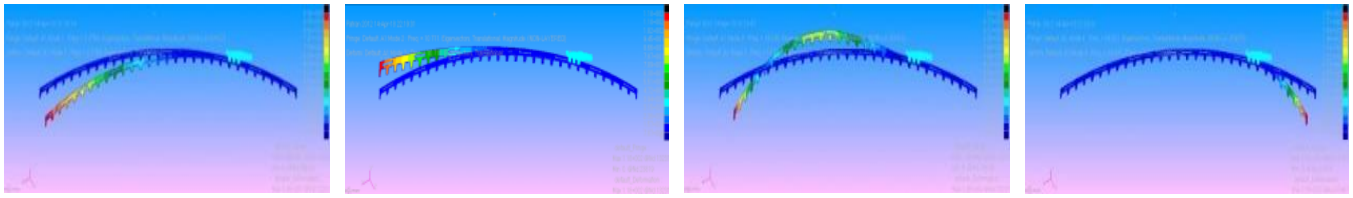

First-order mode Second-order mode Third-order mode Fourth-order mode

c. First four modes of the blade 3

Figure 5 First four modes of blades

3.2.3 Motion analysis of the cutter

(1) Analysis of blade's deformation

When the curved blade is deformed by the constrained of the positioning plate during moving, the motion speed, force and deformation of the blade are complicated, which has an important influence on the plucking speed selection, the blade life, the blade-bud interaction, and the blade clearance setting. Therefore, the kinematics model would be established next section.

According to the structure of the cutter, the double eccentric wheel (the eccentricity is 20 mm) drives the blade to reciprocate in a sine motion in the horizontal plane. With the limitation of positioning plate, the blades deform slightly. This paper considers

the effect of deformation on motion. In view of the symmetry of the blade structure and the motion cycle, the blade was divided into two parts from middle along the blade's length, denoted by A and B separately; also, divided the motion period of the double eccentric shaft into two parts, denoted by T_1 and T_2 separately. Here, just analyzed the deformation of part B.

As shown in Figure 6, the initial time of the blade is located on the circle O_0 where the plate is placed (when the double eccentric shaft that rotates anticlockwise is going to pass the negative y-axis, the blade starts move to right, and start timing) the position shown by the actual arc segment. If there is no positioning plate, then, when time running to t, the blade has moved a distance d_1 to right to the position of the circle O_1; the point X on the blade arrived at the point X_1' at the same time. Supposing that the deformation doesn't change the length of blade's neutral layer, then, limited by the positioning plate, the blade would move a distance d_1 clockwise along the circle O_0, point X moved to point X_1. The drive rules of the double eccentric shaft could be obtained as follow $d_1=s\cos(\pi/2-\omega t)=s\sin\omega t$, where s is half eccentricity of the double eccentric shaft, mm; ω is the angular velocity of the double eccentric shaft, rad/s, t denotes time, s. From Figure 6, it is easy to get the equations of circle O_0, O_1 under the polar coordinates. In Figure 6, θ_1, θ_2 denotes, separately, the angle variation of blade's end point in polar coordinates arise from the motion of distance d_1 and d_2. $\theta_1=d_1/r=s\sin\omega t/r$, where r is the radius of the blade. The coordinates of X_1, X_1' are recorded as (x_1, y_1), (x_1', y_1'), then the function of blade's deformation about t and θ is:

$$\begin{cases}\Delta x = x_1' - x_1 = s\cdot\cos\theta + s\cdot\sin\omega t - r\cdot\cos(\theta - \dfrac{s\cdot\sin\omega t}{r})\\ \Delta y = y_1' - y_1 = r\cdot\sin\theta - r\cdot\sin(\theta - \dfrac{s\cdot\sin\omega t}{r})\end{cases} \quad (2)$$
$$(\pi-1)/2 \le \theta \le (\pi-0.05)/2$$

where, t denotes time, s; θ denotes the angle between the line from point O to the right end of the blade and the X-axis, rad; other parameters are the same as above.

The length of the blade equals to its radius (r=1200 mm) , so the lower bound of θ is (π–1)/2; the blade has a 60 mm long straight segment in the middle on which the connecting bat was connected, hence the upper bound of θ is (π–0.05)/2.

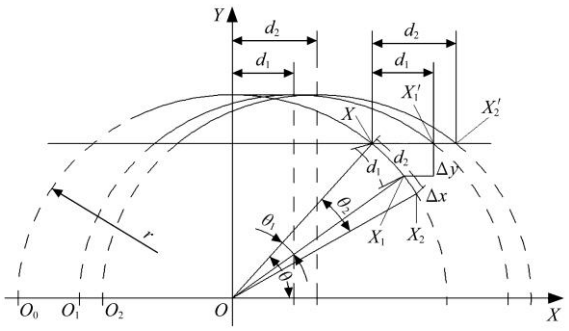

Figure 6 Kinematics model of blade with deformation

It can be seen from Equation (2) that the deformation along the length direction of the moving blade is as follows: the middle portion does not deform, the deformation value satisfies a complex trigonometric function of time and position, and the maximum value increases from the middle to the end, increasing from 0 to 4.984 mm. In order to make the force and wear acted on the blade uniform and meet the principle of equal life, the gap of the positioning bolts (symmetrically distributed along the length of the blade, 4 bolts on either side) should be different depending on the position. The gap of the four positioning bolts on the side of the drive shaft should be increased sequentially. According to the deformation value, it is recommended to take 1 mm, 1.5 mm, 2 mm, 2.5 mm, respectively.

(2) The motion analysis of blade

Combine the drive motion of the double eccentric shaft with the blade's deformation, then have the real motion law of the blade as follow:

$$\begin{cases}x = x_r + x_d\\ = r\cdot\cos\theta + s\cdot\sin\omega t - r\cdot\cos(\theta - (s\cdot\sin\omega t)/r)\\ y = y_r + y_d\\ = r\cdot\sin\theta - r\cdot\sin(\theta - (s\cdot\sin\omega t)/r)\end{cases} \quad (3)$$
$$(\pi-1)/2 \le \theta \le (\pi-0.05)/2$$

where, the subscript r represents rigid, the subscript d represents deformation, and θ, r, w, and t, have the same meaning and range to the one in Equation (2). According to Equation (3), the speed and acceleration of the blade can be obtained at any point:

$$\begin{cases}v_x = \lim\limits_{\Delta t\to 0}\dfrac{\Delta x(\theta, t+\Delta t) - \Delta x(\theta, t)}{\Delta t}\\ = s\cdot\omega\cdot\cos\omega t\{[2 - \sin[\theta - (s\cdot\sin\omega t)/r]\}\\ v_y = \lim\limits_{\Delta t\to 0}\dfrac{\Delta y(\theta, t+\Delta t) - \Delta x(\theta, t)}{\Delta t}\\ = s\cdot\omega\cdot\cos\omega t\cdot\cos[\theta - (s\cdot\sin\omega t)/r]\end{cases} \quad (4)$$
$$(\pi-1)/2 \le \theta \le (\pi-0.05)/2$$

where, v_x and v_y denote the velocity of the blade separately, m/s; Δ denotes the variation of a variable; The other parameters are the same as above.

$$\begin{cases}a_x = \dfrac{\partial v_x(\theta, t)}{\partial t}\\ = \omega^2\cdot s\{(s/r)\cdot\cos^2\omega t\cdot\cos[\theta - (s\cdot\sin\omega t)/r] +\\ \sin\omega t\cdot\sin[\theta - (s\cdot\sin\omega t)/r] - 2\sin\omega t\}\\ a_y = \dfrac{\partial v_y(\theta, t)}{\partial t}\\ = \omega^2\cdot s\{(s/r)\cdot\cos^2\omega t\cdot\sin[\theta - (s\cdot\sin\omega t)/r] -\\ \sin\omega t\cdot\cos[\theta - (s\cdot\sin\omega t)/r]\}\end{cases} \quad (5)$$
$$(\pi-1)/2 \le \theta \le (\pi-0.05)/2$$

where, a_x and a_y denote the acceleration of the blade separately, m^2/s; the other parameters are the same as above.

In order to understand the movement of the blade, the motion model could be visualized when the cutter running at the speed of 900 r/min. It could obtain the variations of the deforming displacement, velocity, and acceleration about the time and space within one motion cycle with Matlab (as shown in Figure 7). From Equations (3)-(5), the blades motion to a complex mixture of sine and cosine functions. Seen from Figure 7, the amplitude of every point on the blade is different from each other although they are about the same, ranging in a trend of concave arc along the right-half blade (the amplitude of the middle points are less than that of two sides). Also, the absolute maximum of the displacement, velocity, and acceleration are 10 mm, 1.0 m/s, 63 m/s^2 respectively. It is easy to obtain the kinematical equation of every point on the blade, only requiring the value of θ belongs to the point.

It can be seen that the speed of every point on the blade is different and time-varying, but the difference is not large. Therefore, it is reasonable to use the average speed of the cutter as the cutting speed factor in the experiment. It can also be seen that during the shearing process, the bud leaves are subjected to the changing inertia force. The kinematics model describes the

cutter's motion more accurately, which affords the possibility to study the attitude and position of the tea shoots while been plucking. They also provide the basis of the dynamic simulation of picking process. Furthermore, the periodic deformation of the blade was given in the model so that fatigue analysis can be carried out to obtain blade's life.

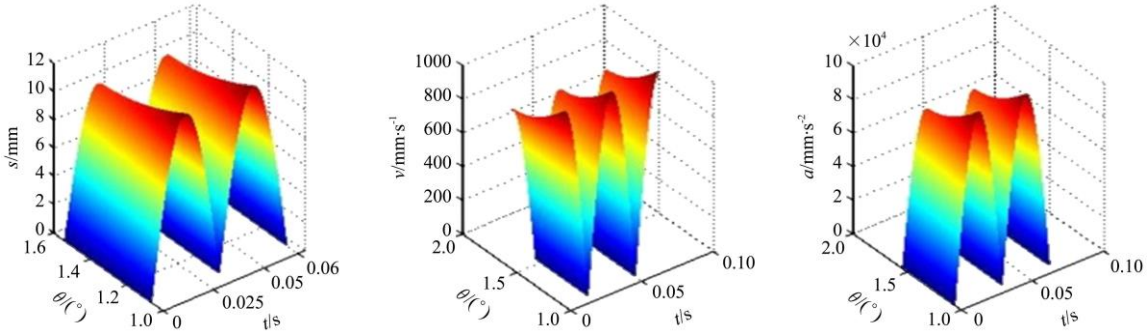

a. Displacement b. Velocity c. Accelerate

Figure 7 Moving rule of the blade

(3) Force analysis of blade

From above analysis, the force exerted on the blades includes shear force and bending moment resulted from deformation, and the inertia force caused by periodic accelerate motion. As they are different from deform part and non-deform part, here we analyze them respectively. In order to obtain the analytic expression of the force and bending moment, simulate the blade with a cantilever beam, as showing in Figure 8.

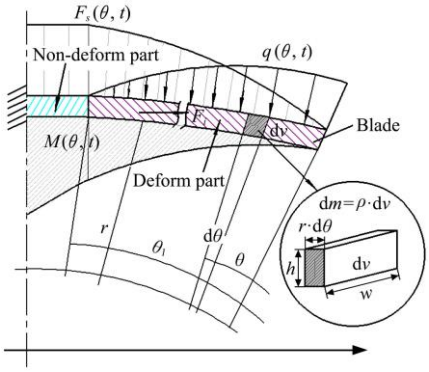

Figure 8 Force analysis of the blade

1) Shear force and bending moment on deform part

From Equation (2), yields the compound deformation as follow:

$$\Delta l = \sqrt{\Delta x^2 + \Delta y^2} \tag{6}$$

According to Hooke theorem, yields distributed load, q:

$$q(\theta,t) = K \cdot \sqrt{\Delta x^2 + \Delta y^2} \tag{7}$$

where, q denotes the distributed load, N/m; K denotes Hooker coefficient, N/m.

Then yields the shear force of deformed part, N:

$$F_s(\theta,t) = K \cdot r \cdot \int_{\frac{(\pi-1)}{2}}^{\theta} \sqrt{\Delta x^2 + \Delta y^2}\,\mathrm{d}\theta \tag{8}$$

And the bending moment of deformed part:

$$M_s(\theta,t) = K \cdot r^2 \cdot \int_{\frac{(\pi-1)}{2}}^{\theta} \int_{\frac{(\pi-1)}{2}}^{\theta} \sqrt{\Delta x^2 + \Delta y^2}\,\mathrm{d}\theta\mathrm{d}\theta \tag{9}$$

2) Inertia force on deform part

As showing in Figure 8, take a minor variation of dθ as analyze objective, we have:

$$\mathrm{d}m = \mathrm{d}v \cdot \rho = \mathrm{d}\theta \cdot r \cdot w \cdot h \cdot \rho \tag{10}$$

where, dm, dv, dθ denote the infinitesimal of mass (kg), volume (m^3), and angle (rad), respectively; r denotes radius of the blade, m; w denotes the width, m; h denotes the thickness, m; ρ denotes the material density, kg/m^3.

And yields the infinitesimal of inertia force in x-axis direction and y-axis direction as follow:

$$\mathrm{d}F_{ix} = \mathrm{d}m \cdot a_x(\theta,t) = r \cdot w \cdot h \cdot \rho \cdot \mathrm{d}\theta \cdot a_x(\theta,t) \tag{11}$$

$$\mathrm{d}F_{iy} = \mathrm{d}m \cdot a_y(\theta,t) = r \cdot w \cdot h \cdot \rho \cdot \mathrm{d}\theta \cdot a_y(\theta,t) \tag{12}$$

where, dF_{ix}, dF_{iy} denote the infinitesimal of inertia force, N. $a_x(\theta, t)$, $a_y(\theta, t)$ are obtained from Equation (5).

The whole inertia force exerted on the deform part is:

$$F_{ixd}(t) = \int_{\frac{(\pi-0.05)}{2}}^{\frac{(\pi-1)}{2}} a_x(\theta,t) r \cdot w \cdot h \cdot \rho \cdot \mathrm{d}\theta \tag{13}$$

$$F_{iyd}(t) = \int_{\frac{(\pi-1)}{2}}^{\frac{(\pi-0.05)}{2}} a_y(\theta,t) r \cdot w \cdot h \cdot \rho \cdot \mathrm{d}\theta \tag{14}$$

where, $F_{ixd}(t)$, $F_{iyd}(t)$ denote the inertia force exerted on deform part separately, N.

3) Force and bending moment on non-deform part

As showing in Figure 8, the force exerted on non-deform part is easy to obtain, the shear force is equal to the $F_s(\theta_1, t)$, θ_1=(π–0.05)/2, the bending moment is linearly varying, which can be written as follow:

$$\begin{aligned} M_{sn}(x,t) &= \int_0^{0.055} F_s(\theta_1,t) \cdot \mathrm{d}x \\ &= \int_0^{0.055} K \cdot r \cdot \int_{\frac{(\pi-1)}{2}}^{\theta_1} \sqrt{\Delta x^2 + \Delta y^2}\,\mathrm{d}\theta\mathrm{d}x \end{aligned} \tag{15}$$

where M_{sn} denotes bending moment, N·m; $x \in [0,0.055]$.

The inertia force exerted on non-deform part arise from the drive motion of the shaft horizontally, therefore,

$$F_{ixn}(t) = a_x(t) \cdot w \cdot h \cdot \rho \cdot l = s \cdot \omega \cdot \cos\omega t \cdot w \cdot h \cdot \rho \cdot l \tag{16}$$

$$F_{iyn}(t) = 0 \tag{17}$$

where, $F_{ixn}(t)$, $F_{iyn}(t)$ denote the inertia force exerted on non-deform part separately, N; s denotes the half eccentricity of the double eccentric shaft, mm; ω denotes the angular velocity of the shaft, rad/s.

Then the total inertial force is the composition of the two parts:

$$F_{ix}(t) = F_{ixd}(t) + F_{ixn}(t) \tag{18}$$

$$F_{iy}(t) = F_{iyd}(t) + F_{iyn}(t) \tag{19}$$

$$F_i(t) = \sqrt{F_{ix}(t)^2 + F_{iy}(t)^2} \tag{20}$$

where, $F_i(t)$, $F_{ix}(t)$, $F_{iy}(t)$ denote the inertia force, the inertia force in x-axis and y-axis that are exerted on the blade, N.

In all, the force exerted on the blade consists of shear force, bending moment and the inertia force. Based on the above analysis, the shear force and bending moment on deformed part were obtained as Equations (8) and (9), the moment on non-deform

part as Equation (15), the total inertial force on whole blade as from Equation (18) to Equation (20), and it's easy to obtain the exact value of force and bending moment if only substitute the parameters with their values, like Δx, Δy, $a_x(\theta, t)$, $a_y(\theta, t)$, ω, r, w, h, s, l.

4 Experiments of physical prototype

4.1 Experimental objective and methods

In order to determine the reasonable value of the main operating parameters (traveling speed, cutter speed and speed ratio) affecting the plucking quality, and improve the quality and efficiency of tea picking, the experiments were carried out in the tea (shrub) garden of Jintan Xinpin Tea Limited Company, Jiangsu Province on July 14 and September 30, 2018 respectively.

a. Plucked tea leaves b. The sample

Figure 9 Experiment effects

Basic situation of tea garden: Longjing 43, planting in strip, curved crown, 0.622 m in height, 0.992 meters in crown width. The yield of this tea garden approximately reached 1.2 t/hm^2. The slope angle is less than 5°. Tea sprouts' density is 97.7/0.1 m^2. The length of the sprout with one bud and three leaves is 7.01 cm and the mass of one hundred sprouts is 106.2 g (the above is the statistical average). The experiment method and the basic situation survey statistical method are implemented in accordance with the standards of tea-plucking machines[30]. Specimens should not less than 100 g. The experiments were carried out on the condition that there was no water on the surface of the tea sprouts.

The experimental instruments and equipment were as follows: self-propelled tea-plucking machine, infrared speedometer, electronic scale, vernier caliper, steel tape, sampling square ruler (size: 0.1 m^2, made of 5 mm wire), sampling bag.

4.2 Experimental design

Three indexes used as the evaluation index set[7] are integrity rate, unpicking rate and stubble unevenness, which will be defined separately below.

(1) The factor level of the single factor experiment was selected according to the empirical data of the hand-held tea plucking machine: Travel speed is 0.3 m/s, the three levels of speed ratio of cutting to traveling are 0.9, 1.0 and 1.2; Speed ratio of cutting to traveling is 1.0, the three levels of travel speed are 0.4 m/s, 0.5 m/s and 0.6 m/s. Every test was repeated 3 times, and every index was tested 3 times.

(2) Design a universal rotary combination experiment of quadratic regression. Factor levels are chosen according to the single factor experiment result[31-33]. Factor levels coding are shown in Table 3. The experiment includes 4 two-level experiments, 4 asterisk experiments and 5 zero-level experiments, totaling 13 groups[34].

In the experiment, the speed ratio of cutting to traveling takes the average value of the reciprocating motion of the rigid body of the blade, and the traveling speed is the move speed of the machine. The travel speed and speed ratio of cutting to traveling have independent hydraulic system, which can be adjusted independently. There are three main indexes to evaluate the plucking quality as follows:

Integrity rate: the mass ratio of intact tea leaf and sprout to the whole sample. In this experiment, the light injury (less than 1/3 damage) and the serious injury (more than 1/3 damage) were classified as non-complete buds, and the target buds were one bud with 2 leaves, one bud with one leaf and single bud.

Unpicking rate: the mass ratio of unpicked tea sprouts in the test point to the sum of the collected sprouts, picked but not collected ones and unpicked ones that picked by hands after the test.

Stubble unevenness: the average of absolute deviations between every stubble's height and their mean (the same reference), as shown in Equation (21)

$$p = \frac{1}{n}\sum_{i=1}^{n}\left|x_i - \bar{x}\right| \tag{21}$$

where, p is stubble unevenness; $\bar{x}$ is the mean of stubbles' height (n>50).

Table 3 Factor levels coding table

Canonical variables	x_j	Variables	
		Travel speed v_m	Velocity ratio λ
$+\gamma$	$x_{j\gamma}$	0.7	1.2
1	x_{j1}	0.64	1.14
0	x_{j0}	0.5	1.0
–1	x_{-j1}	0.36	0.86
$-\gamma$	$x_{-j\gamma}$	0.3	0.8
Variation interval	∇_j	0.14	0.14

4.3 Analysis of results

The experiment data were processed with SPSS and Design-expert.

4.3.1 Single factor experiments

Single-factor experimental results for velocity ratio λ are shown in Table 4. Variance analysis shows that the speed ratio of cutting to traveling has a significant effect on the integrity rate Y_1, unpicking rate Y_2 and stubble unevenness Y_3 at 95% confidence. The optimal factor levels of the speed ratio of cutting to traveling given by Y_1, Y_2, Y_3 are 1.0, 1.2, 1.2, respectively.

Table 4 Single-factor experiment for velocity ratio

Level	Experimental results/%								
	Integrity rate			Unpicking rate			Stubble unevenness		
0.8	49.13	50.36	52.15	2.27	3.33	2.23	6.46	5.97	6.28
1.0	75.65	76.91	78.08	1.63	1.1	1.06	5.07	4.69	4.70
1.2	61.40	63.42	65.27	0.13	0.24	0.11	2.37	1.89	2.53

Single-factor experimental results for travel speed are shown in Table 5. Variance analysis shows that the travel speed has a significant effect on the integrity rate Y_1, unpicking rate Y_2 and stubble unevenness Y_3 at 95% confidence. The optimal factor levels of travel speed given by Y_1, Y_2, Y_3 are 0.5, 0.4, 0.4, respectively.

Table 5 Single-factor experiment for travel speed

Level	Experimental results/%								
	Integrity rate			Unpicking rate			Stubble unevenness		
0.4	68.75	70.57	69.11	0.91	0.77	0.86	2.87	3.23	3.18
0.5	79.94	78.22	76.07	1.17	1.09	1.16	5.08	4.91	4.77
0.6	58.75	56.57	57.11	1.94	1.74	1.62	6.41	6.33	5.90

4.3.2 Universal rotary combination experiment of quadratic regression

According to results in Table 6, the response surface function of Design-expert is used to statistically analyze the experiment result[35,36], and the regression equations of three indexes about two experimental factors were established. The overall significance test results of the model are: The regression model of integrity rate and stubble unevenness is extremely significant, and the regression model of unpicking rate is significant. The results of the misfit test are not significant, and the degree of fitting is good. After removing the insignificant term (at 95% confidence), the regression equation is as shown in Equations (22)-(24). The response surfaces of three experiment indexes are shown in Figure 10.

$$y_1 = 77.17 - 6.72x_1 + 3.97x_2 - 5.11x_1 \cdot x_2 - 8.91x_1^2 - 13.7x_2^2 \quad (22)$$

$$y_2 = 1.55 + 0.75x_1 - 1.47x_2 + 0.55x_2^2 \quad (23)$$

$$y_3 = 2.81 + 1.31x_1 - 2.04x_2 + 0.36x_1^2 + 0.77x_2^2 \quad (24)$$

The comprehensive optimization of three indexes was conducted with software Design expert response surface method.

According to the machine speed range, the common parameters of the hand-held tea plucking machine and the actual conditions of mechanical structure, the range of factor values is as follows: machine speed ranges from 0.3 to 0.7 m/s, speed ratio ranges from 0.8 to 1.2; the range of indexes is as follows: integrity rate ranges from 40% to 100%, unpicking rate ranges from 0.2% to 0.5%, the stubble unevenness ranges from 0.2 to 7 mm. The integrity rate is a large-scale index, and the unpicking rate and the stubble unevenness are small-scale indicators. According to the factor importance for quality indexes, the mass coefficients of integrity rate, unpicking rate and stubble unevenness were chosen separately as follows: 5 (highest), 2, 1 (lowest). The optimal operating parameters of machine are as follow: travel speed is 0.41 m/s, speed ratio of cutting and travelling is 1.06; prediction of three indexes are that integrity rate could be reach to 78.26%, unpicking rate reduced to 0.82%, stubble unevenness reduced to 1.30 mm.

Table 6 Experimental Data of Regression Experiment

Experiment No.		Travel speed x_1	Velocity ratio x_2	Integrity rate y_1/%	Unpicking rate y_2/%	Stubble unevenness y_3/mm
m_c	1	0.64	1.14	39.74	2.12	3.77
	2	0.64	0.86	42.52	5.74	6.83
	3	0.36	1.14	67.79	0.26	0.63
	4	0.36	0.86	50.12	3.08	4.94
m_γ	5	0.7	1.0	57.47	2.76	5.33
	6	0.3	1.0	70.25	1.72	1.48
	7	0.5	1.2	60.27	0.54	1.06
	8	0.5	0.8	48.32	4.31	7.39
m_0	9	0.5	1.0	74.53	1.43	2.63
	10	0.5	1.0	75.68	1.57	2.85
	11	0.5	1.0	78.19	1.65	3.02
	12	0.5	1.0	74.17	1.45	2.57
	13	0.5	1.0	75.28	1.69	2.96

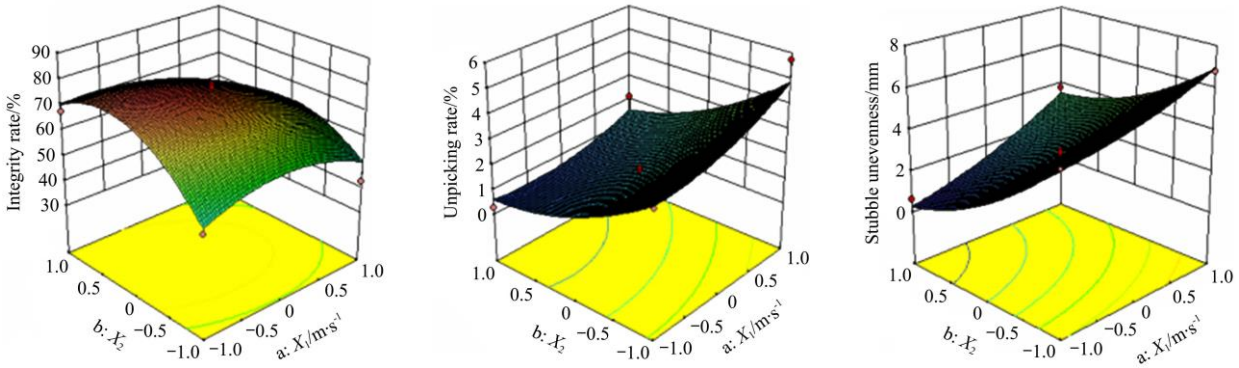

a. Integrity rate b. Unpicking rate c. Stubble unevenness

Figure 10 Response surface of three experiment indexes

4.4 Experimental verification

In the case of the same test conditions, the optimal parameters are tested and verified (time: October 6, 2018, the location and variety are the same as the prototype test) under the optimal parameters, the result of which was that integrity rate could be reach to 77.41%, unpicking rate reduced to 0.87%, stubble unevenness reduced to 1.23 mm. These test indexes that are very close to the predicted values of the regression test. The deviation of the integrity rate of the bud leaves was 1.1%. The ratio of the deviation value was larger due to the small value of the unpicking rate and stubble unevenness, which were 6.09% and 5.38%, respectively. The integrity rate was 7.41% which was higher than the standard, and other indexes meet the requirements. The results show that the optimization results are credible within the optimization parameter index interval.

5 Discussion

Compared with the self-propelled tea plucking machine of Wu[8], this machine has the advantages of ride-on type, lower labor intensity and high productivity. Compared with the results of Wu[8], the integrity rate is 7.74% less, the unpicking rate has a superiority of 1%. For possible reasons for this difference, the analysis is as follows.

(1) Different machine structures. Wu[8] used a single-blade reciprocating cutter and a narrow-width track chassis for traveling between tea trees. This paper proposes a double-blade reciprocating cutter and a cross-teacup traveling track chassis with more uniform cutting speed, more stable motion and more stable chassis movement.

(2) Different operating methods. The tea plucking machine investigated by Wu[8] is a hand-held. When the machine is in operation, it is convenient to observe the relative position of the cutter and the tea crown in real time, the corresponding adjustment can be made in time, which is rather high labor intensity. For the ride-on type tea plucking machine proposed by the paper, it is inconvenient for operator to observe. If the tea crown or the ground suddenly rises and falls, the response speed of the adjustment is not as fast as the hand-held type, which may be an

important factor affecting the quality of tea plucking. However, for tea gardens with flat roads and paths and consistent height of tea crown, the efficiency and operational stability of this machine are very obvious.

(3) Since the stubble unevenness after the mechanized plucking has a great influence on the uniformity of the germination of the next stage, it will affect the consistency and integrity of mechanized plucking next time. Therefore, this paper proposes the "stubble unevenness" as an evaluation index, which is used to characterize the performance of the mechanized plucking and is used as one of the objective functions for comprehensive optimization. Wu[8] did not take this index into consideration.

(4) Different varieties of tested tea trees

Due to the variety of tea, we chose the West Lake Longjing (Longjing 43) as the test tea, which was the top ten famous tea. It is suitable for famous green tea and is representative as a high germination density (in Wu's paper tested tea trees is unspecified). In the future, according to the application requirements, the plucking test of more varieties of tea has a positive significance for promoting the large-scale application of the tea-plucking machine.

6 Conclusions

1) A self-propelled tea plucking machine is presented in this study and the parameters of the chassis and cutter blades are optimized. The machine has excellent performance and the picking height can be adjusted. The machine can be used in the tea garden that has a lengthways slope less than 18°, a crosswise slope less than 20°, and a height of tea trees between 50-120 cm which shows a certain level of automation.

2) The rigid-flex mixed motion model of the reciprocating cutter was established, which indicates that the motion of any point on the blade is the superposition of the sinusoidal reciprocating motion and the deformation of the blade. The deformation of the blade is increased from the symmetrical axial of the blade to the end. Based on the model, the forces exerted on the blade were given by analytical expressions.

3) The test of prototype machine showed that the traveling speed and the speed ratio of cutting to traveling had significant effects on integrity rate, unpicking rate and stubble unevenness. The regression experiment obtained three indexes about the traveling speed and the speed ratio of cutting to traveling. The comprehensive optimal operating parameters are as follow: travel speed is 0.41 m/s, speed ratio of cutting and travelling is 1.06, prediction of three indexes are that integrity rate could be reach to 78.26%, unpicking rate reduced to 0.82%, stubble unevenness reduced to 1.30 mm, the integrity rate could be reach to 77.41%, unpicking rate reduced to 0.87%, stubble unevenness reduced to 1.23 mm. These test indexes that are very close to the predicted values, all surpass the requests specified in the standard of tea plucking with machine. Due to the high integrity rate, combined with the tea grading equipment, it can be applied to the production of famous tea and bulk tea.

Because of structural limitations of the reciprocating cutter, it is inevitable that the some tea sprouts will be broken. The integrity rate of the experiment is the best of the ride-on self-propelled tea plucking machines. This work provides an effective technical equipment for efficient and high-quality mechanized tea picking. In truth, there is still much work to do in the near future, such as making the machines more intelligent, design a multi-parameter test bench, carry out research on multiple factors and carry out research on the influence of tea varieties on picking quality.

Acknowledgements

This work was supported by Research Program: the National Key Research and Development Plan-Research and Investigation of Technology and Equipment for Tea Plucking (Grant No. 2016YFD0701502, China); the Modern Agricultural Technology System of Tea Industry (Grant No. CARS-19, China); The Innovating Program of the Chinese Academy of Agricultural Science, China; Basic scientific research found of Chinese Academy of Agricultural Science (S202005-03), Foundation of Key Laboratory of Modern Agricultural Equipment, Ministry of Agriculture and Rural Affairs, P. R. China.

[References]

[1] Xiao H R, Qin G M, Song Z Y. Study of development strategy to mechanization of tea producing. China Tea, 2011; 7: 8–11. (in Chinese)
[2] Cao W C, Xue Y F, Zhou J G. Study on shearing properties of tea shoot. Journal of Zhejiang Agricultural University, 1995; 21(1): 11–16. (in Chinese)
[3] Lin Y P, Jin X Y, Hao Z L Ye N X, Huang Y B, Tang H Y. Experiment on mechanical properties and crude fiber of tea leaf. Journal of Tea Science, 2013; 33(4): 364–369. (in Chinese)
[4] Bai Q H. Test and study for the cutter of reciprocating-cutting tea-leaf picking machine. Journal of Anhui Institute of Technology, 1985; 15(2): 14–16. (in Chinese)
[5] Jian Y G. Optimum design of tea-leaf picker's cutter system. Journal of Anhui Institute of Technology, 1986; 6(2): 45–47. (in Chinese)
[6] Jin X Y. The optimum velocity of knife and machine of tea plucker and tea pruning machine. Journal of Fujian Agriculture University (Natural Sciences Edition), 1993; 22(4): 470–475. (in Chinese)
[7] Li C H, Gu Q L, He L. Portable double rotary tealeaves plucking machine motion analysis. Research on Agriculture Mechanization, 2011; 35(9): 46–55. (in Chinese)
[8] Terada J.C. Traveling type tea leaf plucking machine. Japan Patent: No. JP2008301831, 2008-12-18.
[9] Terada J. Raveling type tea-leaf plucking machine for sweeping dew. JP2010148519. 2010-07-08.
[10] Sone T. Riding type tea leaf plucking machine. Japan Patent: No. JP2017176022, 2017-10-05.
[11] Yukimaru S. Plucking device of riding type tea leaf plucking machine. Japan Patent: No. JP2016059356, 2016-04-25.
[12] Wu X K. Design and experimental study on self-propelled tea plucking machine. Hefei: Anhui Agricultural University, 2017. (in Chinese)
[13] Xiao H R, Quan Q A. Research on technology and equipment for mechanization of tea garden's working. Beijing: China Agricultural Science and Technology Press, 2012; pp.207–208. (in Chinese)
[14] Xiao H R, Qin G M, Song Z Y, Ding W Q, Han Y. The elevator of tea plucking machine. China Patent, CN 202998865U[P]. 2012-10-19. (in Chinese)
[15] Han Y, Xiao H R, Qin G M, Song Z Y, Ding W Q, Zhao Y. Latest research situations and trends about tea garden machinery in China. Journal of Chinese Agricultural Mechanization, 2013; 34(3): 13–16. (in Chinese)
[16] Wang Z Y, Xiao H R, Ding W M, Qin G M, Song W D, Zhong C Y. Hydraulic system design of chansono walk chassis. Journal of Chinese Agriculture Mechanization, 2010; 5: 72–75 . (in Chinese)
[17] Wu Y P, Yao H X. Engineering machinery design. Beijing: China Communications Press, 2004; pp.176–178. (in Chinese)
[18] Liu W. Research and design of four-tracked cobalt crust mining vehicle chassis for cobalt crusts in the deep sea. Changsha: Changsha Institute of Mining Research, 2018. (in Chinese)
[19] Jiang X. Research on structural design and vibration characteristics of inspection robot chassis. Hefei: Anhui University of Science and Engineering, 2018. (in Chinese)
[20] [20] Chinese Academy of Agricultural Machinery Sciences. Agricultural machinery design manual (Part II). Beijing: China Agricultural Science and Technology Press, 2007; pp.877–959. (in Chinese)
[21] Li Y M, Sun P P, Pang J, Xu L Z. Finite element mode analysis and

experiment of combine harvester chassis. Transactions of the CSAE, 2013; 29(3): 38–46. (in Chinese)

[22] Li Q L, Chen C Y, Ma C Z. Finite element analysis on the modal of the frame of cutting table on 4LYZ-2 rape combine harvester. Transactions of CSAM, 2005; 36(1): 54–56. (in Chinese)

[23] Quan L Z, Tong J, Zeng B G, Chen D H. Finite element mode analysis and experiment of corn stubble harvester. Transactions of the CSAE, 2011; 27(11): 15–20. (in Chinese)

[24] Chen S R, Han H G, Lu Qi. Modal analysis of header for type 4LZ-2.0 combine harvester. Transactions of the CSAM, 2012; 43(Z1): 90–94. (in Chinese)

[25] Li X H, Shen B, Cai Y X, Jiang Y, Zhang K. Model correlation between calculated and experimental mode of 4105 diesel engine crankshaft. Transactions of the CSAE, 2011; 27(11): 51–55. (in Chinese)

[26] Zhang Q, Wang Y, Li B Q, Tian Y. Vibration analysis of a three-drum shearer for a large mining height. Strength of Materials, 2020; 52(2): 160–170.

[27] Sun W, Li R, Jiang J X. Lumped-Parametric Modeling Based on Modal Test and Analysis of Vibration Characteristics of the Hard-Coated Blisk. Journal of Vibration Engineering & Technologies, 2019, 7(4): 347–358.

[28] Farzad E, Mohammad R B. Hygro-thermal vibration analysis of bilayer graphene sheet system via nonlocal strain gradient plate theory. Journal of the Brazilian Society of Mechanical Sciences and Engineering, 2018, 40(9): 1–15.

[29] Wang S Q, Peng P H, Yang Z, Ma Q, Zhang T. Coupling vibration analysis of passenger-vehicle-bridge system. Journal of Vibration Engineering, 2018; 31(1): 30–38. (in Chinese)

[30] JB/T 6281.2—1992, Standards of machinery industry of the People's Republic of China-Test Method for Tea Plucking Machine. Beijing: China Machine Press, 1992. (in Chinese)

[31] Gao X J, Zhou J H, Lai Q H. Design and experiment of pneumatic cylinder precision seed-metering device for panax notoginseng. Transactions of the CSAE, 2016; 32(2): 20–28. (in Chinese)

[32] Xu L M, Chen J W, Wu G, Yuan Q C, Ma S, Yu C C. Design and operating parameter optimization of comb brush vibratory harvesting device for wolf berry. Transactions of the CSAE, 2018; 34(9): 79–81. (in Chinese)

[33] Wang X Y, Liang J, Shang S Q, Jiang J T, Yang R B. Design and experiment of half feeding type peanut picker. Transactions of the CSAE, 2008; 24(9): 94–98. (in Chinese)

[34] Wang W Z. Design and analysis of experiments. Beijing: High Education Press, 2011; pp. 9–22, 115–143. (in Chinese)

[35] Zhou F J, Lu J, Du J X. Parameters optimization and experiment of corn-paper transplanting machine with seedling disk. Transactions of the CSAE, 2014; 30(1): 18–24. (in Chinese)

[36] Tian S B, Yang J F, Wang, R L, Xu D L, Li T L. Optimization experiment of operating parameters on vibration sorting-clip. Transactions of the CSAE, 2014; 30(6): 9–16. (in Chinese)